JOURNAL OF CATALYSIS 97, 85–99 (1986)

Effect of Titania Oxidation State on the Chemisorptive Properties of Titania-Supported Nickel

G. B. RAUPP[1] AND J. A. DUMESIC[2]

Department of Chemical Engineering, University of Wisconsin, Madison, Wisconsin 53706

Received April 24, 1985; revised August 19, 1985

Temperature-programmed desorption (TPD) under ultrahigh vacuum conditions and transmission electron microscopy (TEM) were used to characterize the adsorption behavior of CO and H_2 on low-surface-area samples prepared by depositing nickel onto titania films. The effect of titania oxidation state on CO adsorption from Ni was probed by studying 0.2-nm Ni overlayers deposited *in situ* on titania surfaces vacuum-annealed at successively higher temperatures to vary the oxygen-to-titanium ratio from 2 to 1. The CO adsorption strength and saturation coverage on Ni decreased with increased extent of titania reduction. These effects could be attributed to electronic metal–support interaction between Ni and underlying titania in the absence of titania adspecies on the Ni surface. This type of interaction becomes unimportant for Ni overlayers or Ni crystallites thicker than about 3 atomic layers. The strength of CO adsorption was also found to be dependent on the initial nickel overlayer thickness for samples reduced at 650 K in hydrogen at 10^{-3} Pa. The desorption peak temperature increased from 360 K for a 0.2-nm Ni overlayer to 420 K for a 2.5-nm Ni overlayer. It is proposed that the thinner nickel overlayers lead to smaller nickel particles during this treatment in hydrogen and that these smaller particles are more completely covered by titania adspecies from the support. Transmission electron micrographs suggested that the supported Ni crystallites develop a raft-like morphology upon reduction. The Ni particles were relatively resistant to sintering. Dissociative CO adsorption on the model nickel/titania surfaces was not observed under any conditions, suggesting that the Ni crystallites adopt flat morphologies and that sites active for CO dissociation under ultrahigh vacuum conditions are not created at nickel/titania interfaces.

INTRODUCTION

An important difference between catalyst supports such as titania and conventional supports such as silica, alumina, or magnesia is that the former materials are reducible under high-temperature, reducing conditions. At issue is the role of partially reduced titania (e.g., Ti^{3+}) in the manifestations of so-called "strong metal–support interactions" (SMSI) for titania-supported Group VIII metal catalysts. Potential roles of reduced titania include the following: (a) creation of a driving force for spreading of the supported metal particles over the support surface to form thin, two-dimensional crystallites, or "rafts" (e.g., (*1, 2*)); (b) charge transfer from Ti^{3+} to the metal particles, which saturates the unfilled *d*-orbitals of the surface metal atoms and inhibits subsequent chemisorption of H_2 and CO (e.g. (*3–5*)); (c) creation of special interfacial sites, consisting of a metal atom, a Ti^{3+} cation, and an anion vacancy, which enhance the CO dissociation rate in CO hydrogenation reactions (*6–8*); and (d) modification of the mobility of either titania or the metal particles to allow migration of titania moieties onto the surfaces of the metal particles (e.g. (*2, 9–11*)).

In this paper we investigate the role of titania oxidation state on the chemisorptive behavior of model-supported nickel crystallites. The following strategy was employed. Reproducible surface oxidation states of titanium on a clean polycrystalline foil were

[1] Present address: Department of Chemical and Bio-Engineering, Arizona State University, Tempe, Ariz. 85287.

[2] To whom correspondence should be addressed.

0021-9517/86 $3.00

created through vacuum annealing at various temperatures (*12*). Nickel was then deposited *in situ* on the titania surface through vacuum evaporation. Using temperature-programmed desorption (TPD), chemisorption of CO and H_2 were studied on these surfaces. Parallel *ex situ* electron microscopy examination allowed characterization of the nickel particle size distribution and morphology.

Few studies of model-supported catalysts combining temperature-programmed desorption and electron microscopy characterization have been reported in the literature. Ladas *et al.* (*13*) have investigated the adsorption and oxidation of CO on Pd/Al_2O_3 model-supported catalysts. Chemisorption of CO was found to depend on the average Pd particle size measured by TEM, with adsorption strength decreasing with decreasing particle size. Doering *et al.* (*14*) studied the interaction of CO with small nickel particles supported on mica. Molecular desorption was accompanied by dissociation of CO. Dissociation probability increased with decreasing particle size. Electron microscopy further showed that exposure to CO followed by thermal treatments caused morphological particle changes which were most severe for the smallest particles. Changes in particle size and crystal habit were accompanied by shifts in the CO binding strength. These results emphasize the need for physical characterization of model-supported metal crystallites in conjunction with chemisorptive or catalytic measurements.

EXPERIMENTAL

Temperature-programmed desorption experiments were performed in the UHV chamber described previously (*15, 16*). A constant heating rate of ca. 20 K $\cdot$ s^{-1} was used throughout. Model titania surfaces of varying oxidation state were created *in situ* by vacuum-annealing a clean, oxidized titanium polycrystalline foil (Alfa, 99.98%) at temperatures from 300 to 800 K (*12*). Characterization with X-ray photoelectron and Auger electron spectroscopies revealed that samples treated in this manner had surface O/Ti ratios decreasing smoothly from ca. 2.0 to 1.1 as the annealing temperature was increased from 300 to 800 K (*12*).

Nickel was evaporated *in situ* from an alumina crucible held at 1625 K; typical deposition rates were 0.05 nm $\cdot$ s^{-1} as measured with a calibrated quartz crystal thickness monitor. Following extended outgassing at temperatures higher than 1500 K prior to deposition, background pressure did not increase above 3×10^{-7} Pa during deposition. Between each deposition, nickel was removed from the titania surface by several sputter–anneal cycles. This successfully removed all nickel as judged by CO thermal desorption from the sputter-cleaned surface.

Model-supported nickel samples suitable for transmission electron microscopy were prepared using the method previously described by Tatarchuk and Dumesic (*17*). In short, a 0.025-mm-thick titanium foil (Caesar, 99.95%) was treated in oxygen at 620 K for 2 h. This produced a ca. 30-nm-thick film of rutile TiO_2. The titanium metal backing was etched away in acid solution and the thin oxide film placed on titanium electron microscopy grids prior to nickel deposition, which was subsequently carried out in the TPD chamber under the conditions described above. Treatments in hydrogen (atmospheric pressure) were carried out *ex situ* in a quartz cell for 1 h at various temperatures. The samples were cooled in hydrogen, evacuated, and then passivated with a flowing O_2/He mixture (ca. 5 vol% O_2) for 30 min.

Transmission electron microscopy studies of these samples were performed using a JEOL 100B instrument operated at 100 kV with a 30-μm objective aperture inserted for contrast. Magnifications were calibrated using carbon replica gratings. Reported particle size distributions were determined from a minimum of 800 crystallites (maximum 1200) for each sample.

RESULTS

CO Thermal Desorption

Carbon monoxide desorption from model-supported nickel on titania was found to depend on the initial nickel overlayer thickness. Figure 1 illustrates this behavior. Carbon monoxide desorption flux spectra from CO saturation coverages are shown for initial thicknesses ranging from 0.2 to 2.5 nm on a titania surface "annealed" under vacuum at 300 K (fully oxidized surface). The surfaces were treated at 650 K for 120 s in 3×10^{-4} Pa H_2 following deposition of nickel; this was found to be necessary to obtain a reproducible desorption spectra from the surfaces. Note that this treatment should reduce the titania as reported in another publication (*12*). For a 0.2-nm Ni layer, the smallest Ni thickness studied, CO desorbed in a manner similar to desorption from Ni surfaces containing large amounts (i.e., ca. 0.7 monolayer equivalent) of titania (*18*). In addition to desorption from titania sites at ca. 200 K (*12*), desorption from Ni sites occurred from a broad distribution of binding energies centered near 360 K. As the nickel thickness was increased, the following changes in desorption behavior were observed: (a) population of the titania adsorption states decreased, (b) population of the nickel adsorption states increased, and (c) overall CO adsorption strength on nickel increased as evidenced by the increase in the main desorption state peak temperature to 420 K. At the largest Ni overlayer thickness, 2.5 nm, the overall desorption trace is similar to the CO desorption traces from a clean Ni polycrystal (*18*). The average adsorption strength, however, is slightly less for the titania-supported nickel crystallites. For first-order desorption kinetics and a preexponential of 10^{16} s^{-1}, a CO desorption activation energy of 127 kJ · mol^{-1} can be estimated, compared to the value of 134 kJ · mol^{-1} (*18*) from the clean nickel surface. Saturation coverage was ca. 90% of the value on the clean nickel surface.

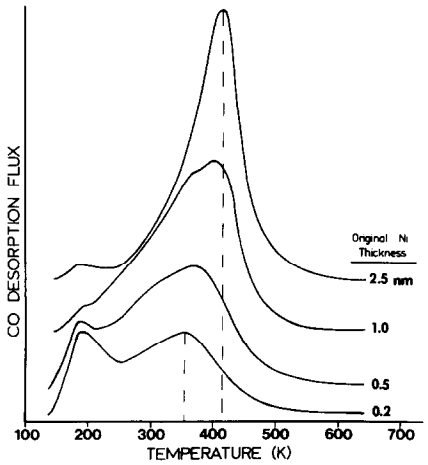

FIG. 1. CO desorption from titania surfaces containing different amounts of Ni as indicated. Initial CO coverages were at saturation.

Assuming that nickel deposited on titania follows the generally observed trend for vacuum-evaporated overlayers in which average metal particle size increases with amount deposited (e.g. (*14*)), these results show a strong dependence of CO adsorption strength on average metal particle size. What remains unclear, however, is to what extent migration of titania species onto the supported particles during thermal treatment may be responsible for the weaker adsorption observed; therefore, the following experiment was performed. A constant amount of Ni, 0.2 nm ± 10%, was deposited onto titania preannealed under vacuum at various temperatures to give different oxidation states of the titania surface (*12*). The titania substrate was held at ca. 250 K during deposition of nickel to minimize diffusional processes. Immediately following deposition, the sample was cooled to below 170 K (this took ca. 60 s) and saturated with carbon monoxide. Subsequent thermal desorption spectra (at least for the first heating cycle) were therefore representative of small particles or a thin (ca. 1 atomic layer) film of Ni on an underlying substrate of titania. In this manner the chemical effects of *underlying* reduced versus oxidized titania on small nickel particles could be studied.

Figure 2 compares these initial CO desorption spectra for nickel on titania for different titania vacuum preannealing temperatures. Surfaces preannealed at temperatures lower than or equal to 450 K, which are the most oxidized titania surfaces, exhibited essentially identical initial CO desorption behavior. The majority of the CO desorbed as a broad peak centered at ca. 390 K, with a lesser contribution near 260 K as evidenced by the shoulder on the low-temperature side of the major peak. For surfaces annealed at higher temperatures up to 650 K, this shoulder became somewhat more pronounced. Nonetheless, the overall CO adsorption strength and saturation coverages were nearly identical to the corresponding values for more-oxidized titania. It should be noted that the absence of CO desorption from temperature regions (150–200 K) characteristic of titania sites indicates that the deposited nickel overlayers are essentially contiguous and cover the entire titania surface.

Desorption from the surface preannealed at 720 K exhibited both a slight weakening of adsorption strength and a slight decrease in saturation coverage compared to the surfaces preannealed at lower temperatures. This was accompanied by a small contribution due to CO desorption from titania

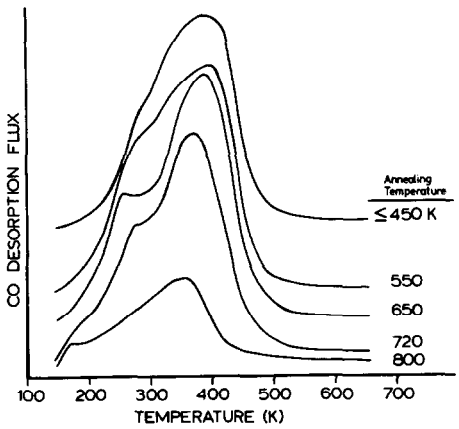

FIG. 2. Initial CO desorption immediately following deposition of 0.2-nm Ni on titania surfaces preannealed at different temperatures. CO exposures were 50 L at 150–170 K.

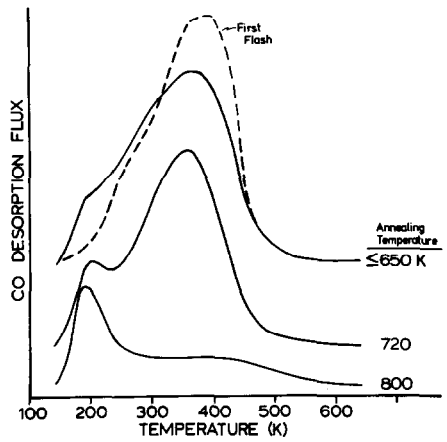

FIG. 3. CO desorption spectra following heating to 650 K of titania surfaces initially annealed at indicated temperatures and with 0.2 nm of deposited Ni. CO expsoures were 50 L at 150 K.

sites. For the surface preannealed at 800 K, a further decrease in adsorption strength was observed accompanied by a significantly lower saturation CO coverage attributable to chemisorption on nickel. It appears, therefore, that *underlying* reduced titania modifies nickel to a greater degree than does oxidized titania for *thin* Ni crystallites or layers of the same approximate thickness.

Effect of Thermal Treatments on CO and H_2 Desorption

Following the initial heating during TPD of the thin Ni overlayers on titania substrates preannealed at different temperatures (see Fig. 2), CO desorbed during subsequent flashes in a somewhat different manner, as shown in Fig. 3. The maximum temperature achieved in the first flash was 650 K; for a heating rate of 20 K · s^{-1} and utilizing liquid nitrogen, the sample temperature exceeded 450 K for about 30 s. Nonetheless, this short thermal treatment resulted in significantly different CO desorption behavior between first and second flashes. For all nickel-containing surfaces originally anneal at temperatures ≤650 K, desorption traces were identical, with the CO desorption peak maximum

during the second TPD flash shifted to a slightly lower temperature and broadened about the maximum relative to the first flash. Population of the nickel states decreased to ca. 80% of the values obtained from the first adsorption/desorption cycle. This was accompanied by a measurable population of CO adsorbed on sites characteristic of titania.

Similar behavior was observed for the surface preannealed at 720 K. For the 800 K surface, a more dramatic shift in site populations was evident. In addition, CO binding energies were broadened to a distribution of sites that included strengths as high as those characteristic of clean nickel (desorption temperatures near 450 K).

Third and subsequent adsorption/desorption cycles did not further alter CO desorption behavior. Over the course of many flash desorptions (i.e., 30–40) small decreases in total saturation coverage on nickel-like sites were observed. Additional studies using TPD and electron microscopy were employed to determine the origin of this reduction in chemisorption capacity, and these will be outlined later in this paper. Note that Chung and co-workers (*19, 20*) have reported that nickel deposited on single-crystal TiO_2 diffuses into the bulk oxide during heating at temperatures higher than 573 K.

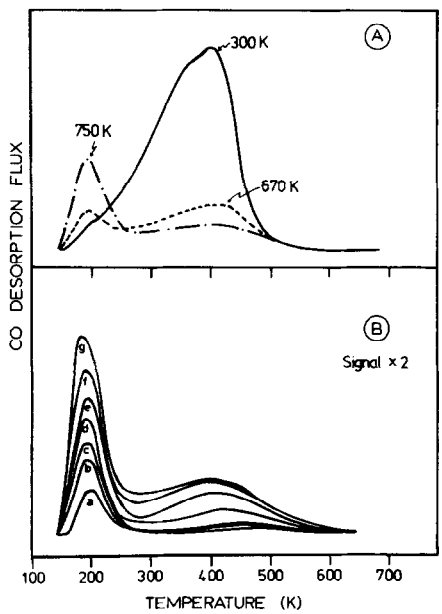

FIG. 4. Effect of heating 1-nm Ni on titania in low-pressure hydrogen at different temperatures. (A) Comparison of CO desorption from saturation coverages; (B) CO desorption from the surface reduced at 750 K following different CO exposures at 150 K: (a) 0.2, (b) 0.4, (c) 0.8, (d) 1.2, (e) 2.5, (f) 5.0, and (g) 20 L.

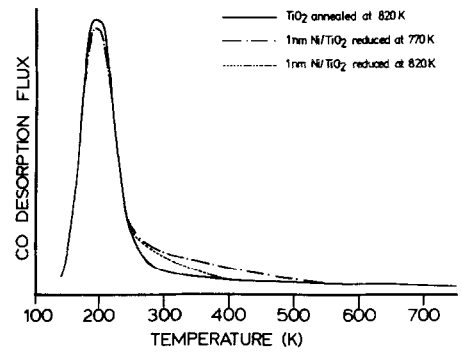

FIG. 5. Effect of heating 1-nm Ni on titania at high temperatures in low-pressure hydrogen on CO desorption from saturation coverages.

The effect on CO desorption behavior of heating a titania thin film containing 1-nm Ni in 1×10^{-3} Pa H_2 for 600 s at increasing temperatures is shown in Figs. 4 and 5. Figure 4A compares CO desorption (initial flashes) from saturation coverages for the untreated Ni/titania surface (300 K) and from surfaces reduced at 670 and 750 K. Following reduction at 670 K, CO saturation coverage on Ni sites (desorption temperatures higher than 250 K) decreased from 82% of the clean polycrystalline nickel foil value for the unheated surface to 27% of this value. Heating in low-pressure hydrogen at 750 K further decreased saturation coverage to 15% of the value obtained for the clean nickel foil.

Weakening of CO adsorption on all Ni sites was not observed following thermal treatment; on the contrary, the major effect of heating in hydrogen appears to be loss of Ni surface area. This loss of area is thought to occur primarily through breakup of the contiguous nickel film and nucleation into discrete particles for pretreatment tempera-

tures of ca. 700 K or lower, as confirmed by the electron microscopy results to be discussed later. At higher pretreatment temperatures, migration of titania adspecies onto the surfaces of the nickel particles could also decrease available surface area through site-blocking (*15, 18*). Based on the CO desorption peak temperatures reported elsewhere (*18*) for various submonolayer coverages of titania on nickel, we conclude that, if titania adspecies are present on the model-supported nickel crystallites following reduction at 670 K, their concentration is low (i.e., ≤ 0.1 monolayer).

Evidence for the presence of titania surface species on nickel is provided by the behavior of CO adsorption state filling with increasing CO exposure following hydrogen reduction, as illustrated in Fig. 4B for the surface treated at 750 K and dosed with different amounts of CO (1 L = 1.3×10^{-4} Pa · s). The rates at which the respective titania ($T_p \sim 190$ K) and nickel states ($T_p \sim 400$ K) fill suggest that the initial sticking coefficient for CO adsorption has been decreased from the value of unity measured for the clean nickel foil. If initial sticking coefficients, S_0, were those measured on clean nickel (1.0) and reduced titania (0.2), and 15% of the total exposed surface is nickel (based on the areas under the CO desorption peaks), then the respective populations of the nickel and titania states should initially fill at approximately the same rate. This was clearly not observed. Instead, the titania state filled to about one-third of saturation coverage before significant population of the nickel sites was observed. This decrease of the CO sticking coefficient on nickel can be related to the presence of titania on the Ni surface. Based on sticking coefficient measurements for titania-containing nickel surfaces (*18*), and assuming that titania adspecies are uniformly distributed over the surfaces of the nickel particles, we estimate an average titania adspecies concentration of 0.2 monolayers for samples treated at 750 K.

Heating the nickel on titania samples at temperatures higher than 750 K further decreased the CO saturation coverage on nickel, as shown in Fig. 5. Desorption traces from the sample treated at 770 and 820 K are compared to that from a nickel-free titania surface annealed at 820 K. It is apparent that the saturation CO coverage on nickel sites and the average adsorption strength are lower on the nickel–titania samples, compared to samples treated in H_2 at temperatures lower than 750 K. *Ex situ* XPS analysis of the surface suggested that the majority of this loss in CO adsorption capacity was caused by significant loss of nickel surface area.

Hydrogen adsorption/desorption was also studied on the 1-nm Ni on titania model-supported catalyst as a function of low-pressure hydrogen reduction temperature. Figure 6A shows that H_2 desorption from a 1-nm Ni layer on titania is similar to desorption from a clean polycrystalline Ni foil (*18*). Note that for these experiments the sample had been flashed ca. 10 times to 650 K (during CO desorption experiments)

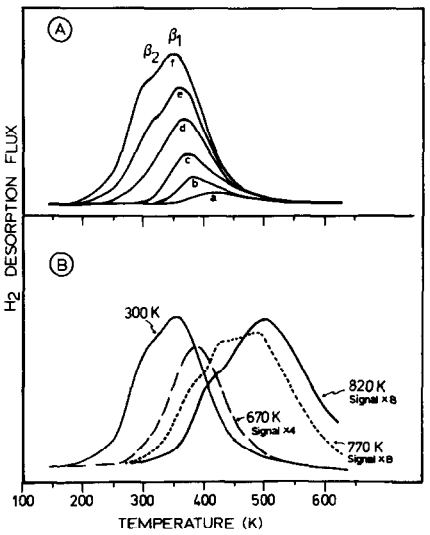

FIG. 6. (A) Hydrogen desorption from 1-nm Ni on titania following different H_2 exposures at 150 K: (a) 0.4, (b) 1.0, (c) 3.0, (d) 6.0, (e) 12, and (f) 20 L. (B) Effect of heating in low-pressure H_2 at different temperatures (indicated) on desorption from saturation coverage. Sample dosed with hydrogen at 300 K followed by cooling in hydrogen to 150 K.

but had not been heated at elevated temperature for extended time. Two desorption states were evident. These states compare well in desorption energy with the β_1 and β_2 states assigned to the clean nickel surface. Moreover, the ratio of the saturation coverages of CO to H_2 on the Ni/titania surface was nearly identical to that for the polycrystalline Ni foil.

Thermal treatment in low-pressure hydrogen (1×10^{-3} Pa) at successively higher temperatures resulted in decreased values for H_2 saturation coverage and increased average H_2 adsorption strength, as depicted in Fig. 6B. (These spectra were obtained after extended dosing of hydrogen at 300 K followed by cooling the sample in hydrogen to about 150 K.) After treatment at 670 K, the saturation hydrogen coverage was markedly lowered, with the most severe decrease for the lower-temperature, or β_2-H state. The observed increase in peak temperature for the β_1-H state can be attributed to a lower initial saturation coverage. Significant increases in adsorption strength were observed for sample reduction temperatures equal to or above 770 K, where filling of higher temperature, activated adsorption states (peak temperatures ca. 500 K or higher) became important. Note that filling of the activated states required extended exposures at elevated dosing temperatures (i.e., 300 K) (*15, 18*).

The dependence of the ratio of CO to H-atom saturation coverages as a function of reduction temperature is shown in Table 1. This table reveals that the decrease in hydrogen saturation coverage is more severe than the corresponding decrease in CO coverage as reduction temperature is increased to 750 K. This trend is similar to that observed for increasing coverage of titania on nickel determined previously (*18*); saturation coverages for those surfaces are included in the table for comparison. For treatment temperatures of 770 K and higher, activated hydrogen adsorption states (the contribution from these states was not included in Table 1) fill and reverse this trend. For example, the CO : H ratios including activated hydrogen adsorption states for the surface treated at 770 and 820 K were 0.88 and 0.79, respectively. The fact that the CO : H ratio for the model-supported nickel including activated states was not significantly lower than the value on the clean nickel foil suggests that if the activated H_2 adsorption states are associated with titania, as previously postulated (*15, 18, 21*), then spillover from nickel to titania is limited to titania near or on the nickel particles under the UHV-TPD conditions of this study. Similar conclusions have been made for high-surface-area catalyst samples (*21, 22*).

TABLE 1

Dependence of CO and H Saturation Coverages[a] on Titania-Supported Nickel as a Function of Reduction Temperature; and Data for Nickel Surfaces Containing Different Coverages of Titania Included for Comparison[b]

Surface	Treatment temperature (K)	θ_{CO}	θ_H	θ_{CO}/θ_H
1-nm Ni/TiO_2	300	0.55	0.66	0.83
	670	0.18	0.12	1.5
	750	0.10	0.04	2.5
	770	0.067	0.02	3.4
	820	0.034	0.01	3.4
	Titania coverage (equivalent monolayers)			
Polycrystalline Ni	0	0.67	0.94	0.71
	0.10	0.64	0.64	1.0
	0.19	0.53	0.38	1.4
	0.28	0.43	0.23	1.9
	0.69	0.19	0.07	2.7

[a] Does not include activated hydrogen states.
[b] From Ref. (*18*).

Effect of Thermal Treatments on Nickel Morphology

Transmission electron microscopy studies of nickel particles on thin titania films allowed examination of the changes in nickel morphology as a function of reduction temperature. A transmission electron micro-

graph of a blank titania film is shown in Fig. 7. Micrographs of a titania film covered with 1-nm Ni, but not heated above 300 K, were essentially identical. Although detectable structure was evident in both samples including dark features of dimensions greater than 10 nm, discrete Ni crystallites were not formed during the initial deposition of the 1-nm Ni overlayer.

The electron micrographs in Figs. 8A and B show the representative changes in Ni particle morphology for specimens after treatment in hydrogen at temperatures up to 820 K. Figure 9 presents corresponding particle size distributions. Reduction at 650 K leads to a rather uneven distribution of particle sizes, with significant areas covered by relatively large particles in the range 5–7 nm, and remaining areas containing many smaller particles in the range 1–3 nm. The larger particles apparently break up into smaller particles upon reduction at 750 K leading to a more uniform particle size distribution. Reduction at 820 K leads to an increase in the average particle size from ca. 2.0 to 2.5 nm. There was very little change in particle morphology between reduction temperatures of 650 and 820 K. For samples treated at both low and high temperatures, many of the Ni crystallites are irregularly shaped and have faceted outlines. Across a given particle, the electron scattering density is relatively uniform, suggesting that the particles have a flat rather than hemispherical shape. The appearance of the particles did not change when the samples were tilted through 35° from the normal to the incident electron beam.

Flat or raft-like particles have previously been observed for Pt (*1*) and for Ni (*2*) particles on titania thin films. Evidently a driving force exists under reducing conditions to maximize the metal–titania interfacial area. This driving force is thought to be responsible for both raft formation and for the breakup of large particles to give smaller particles and a more uniform size distribution during reduction at 750 K.

No significant loss of nickel from the titania surface, other than that amount that can be accounted for through moderate particle sintering, is apparent even at 820 K, the highest reduction temperature employed. Estimates of the total nickel areas from electron micrographs revealed a loss of only ca. 20% of the original Ni area between reduction at 650 and 820 K, whereas treatment of the TPD samples at these temperatures resulted in an 80% decrease in saturation CO coverage. Simoens *et al.* (*2*) reported that reduction of similar low-surface-area Ni/TiO_2 samples must be carried out at 973 K to observe significant loss of nickel from the surface. Loss of nickel, presumably through diffusion into the oxide matrix, was accompanied by significant particle sintering and transformation from raft-like to three-dimensional, hemispherical Ni particles.

DISCUSSION

The CO TPD measurements on model nickel titania-supported catalysts showed that CO adsorption behavior is a function of nickel particle size, oxidation state of the support, and pretreatment severity. Hydrogen TPD measurements showed that suppression of hydrogen adsorption capacity on Ni is more severe than suppression of CO capacity for identical treatment conditions. Severe loss of adsorption capacity (for nonactivated states) was observed for reduction temperatures greater than or equal to 770 K. Complementary electron microscopy studies of nickel on thin titania films suggested that the nickel particles are relatively stable during reduction in H_2 at temperatures up to 820 K.

The results described above yield information on the possible roles of electron transfer (as inferred from TPD-derived adsorption strengths), raft formation, special interfacial site formation, and diffusional processes with regard to so-called strong metal–support interactions. Although these issues are not independent, they are discussed separately below for clarity.

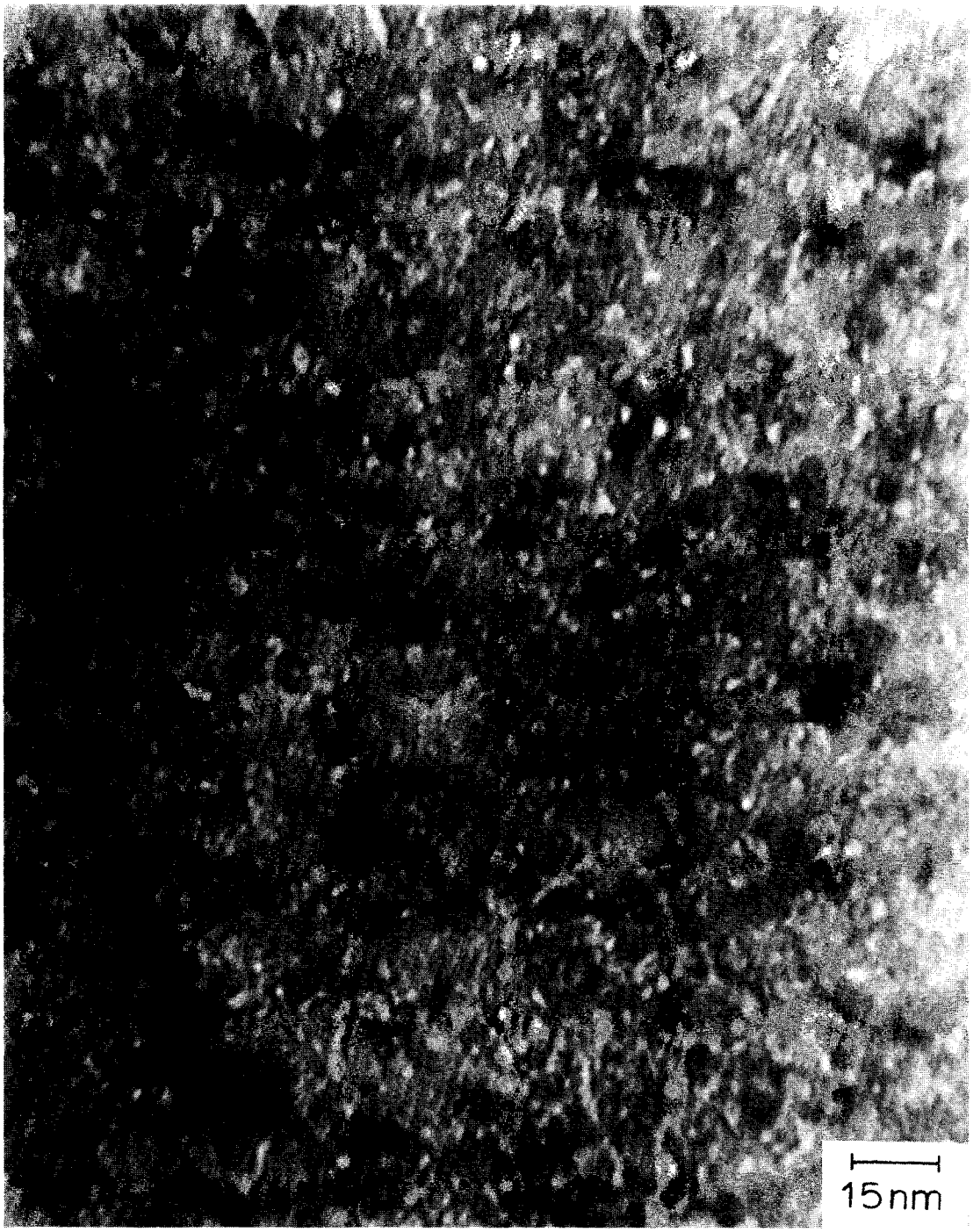

FIG. 7. Transmission electron micrograph of blank titania.

Evidence for Electron Transfer

The CO TPD spectra in Fig. 2 provide evidence for electron transfer between titania and supported nickel particles *in the absence* of titania species on the surfaces of the metal crystallites. The saturation CO coverage and average desorption energy

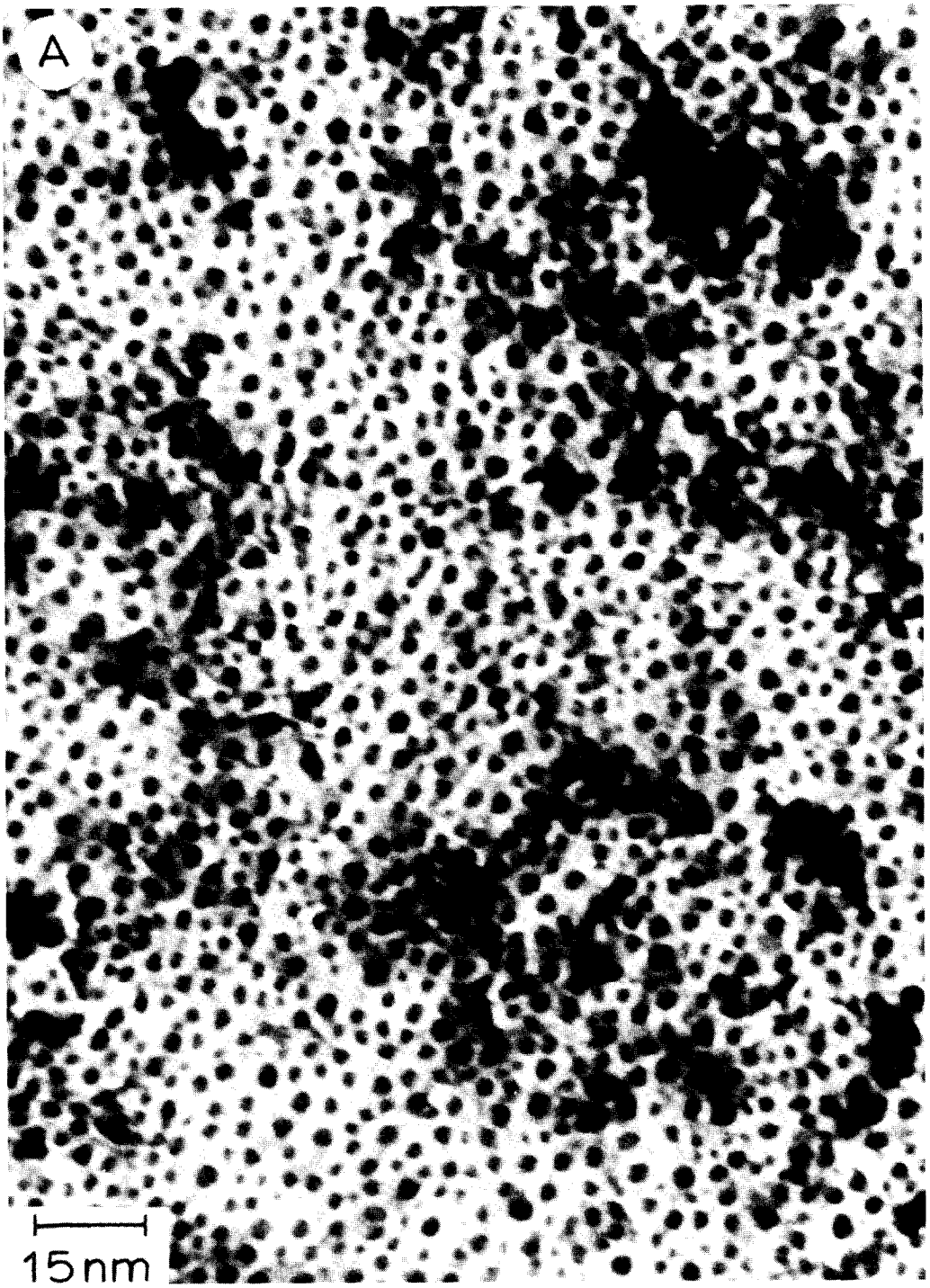

FIG. 8. High-magnification transmission electron micrographs of 1-nm Ni on titania reduced in flowing H_2 for 1 h at (A) 650 K and (B) 820 K.

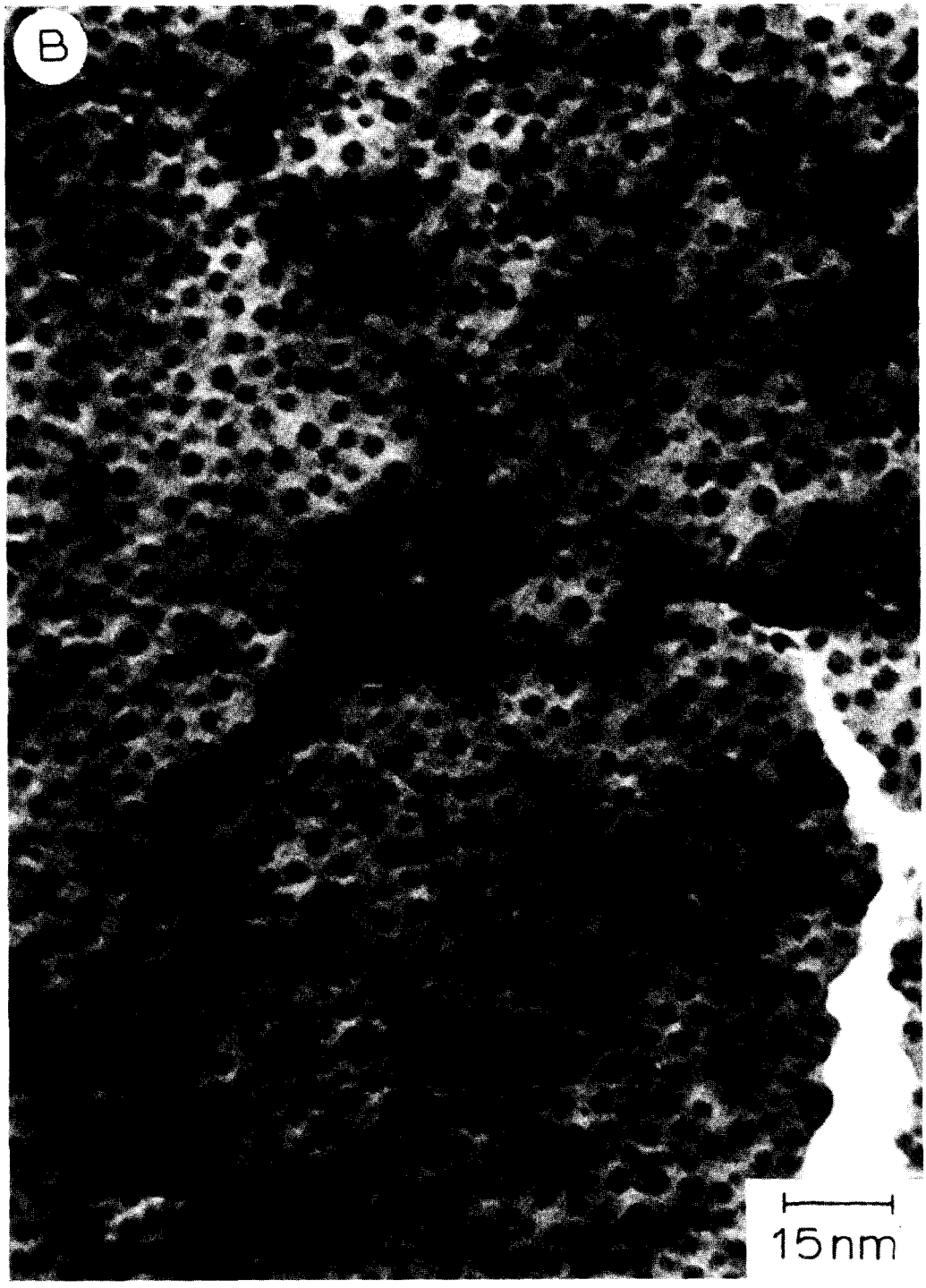

FIG. 8—*Continued.*

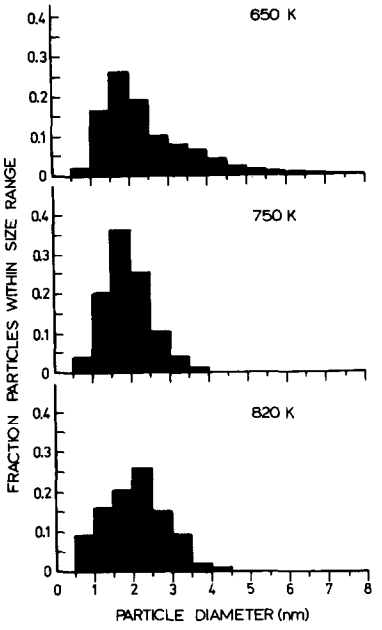

FIG. 9. Particle size distributions of nickel crystallites from transmission electron micrographs of 1-nm Ni on titania reduced in flowing H_2 for 1 h at 650 K, 750 K, and 820 K.

decreased for desorption from a 0.2-nm Ni overlayer immediately following Ni deposition (i.e., prior to heating the sample) on titania surfaces prereduced to increasing extents. Note that in the absence of nickel agglomeration during deposition, this amount of nickel corresponds to a continuous layer ca. one monolayer thick. The extent to which agglomeration occurred is not precisely known, but it is thought to be minimized by holding the oxidized titanium foil at 250 K during deposition. This presumption was supported by electron microscopy examination of untreated 1-nm Ni on titania films which failed to reveal discrete crystallites and by the CO TPD spectra which showed little or no contribution from titania adsorption sites for the titania surfaces preannealed at temperatures less than or equal to 650 K. The CO desorption traces during the first flash consisted of a broad, high-temperature peak near 390 K and a low-temperature shoulder near 240–270 K. This behavior, most notably the presence of the low-temperature shoulder, is markedly different from the behavior of CO desorption from titania-containing nickel foils (*18*) and can be taken as evidence for charge transfer between the underlying titania and the thin nickel layer.

For titania surfaces preannealed at 720 or 800 K, CO adsorption strength and capacity are reduced further, compared to the sample preannealed at 650 K. Because the corresponding CO desorption traces contain minor contributions from CO adsorbed on titania sites, it is thought that during the Ni deposition process some agglomeration of nickel, as well as diffusion into the bulk, might occur during deposition despite the low substrate temperature. Chung *et al.* (*20*) have shown that nickel deposition on single-crystal titania generates surface Ti^{3+}-anion vacancy sites.

A portion of the apparent metal–support interaction described above may be due to inherent structure sensitivity of CO adsorption on nickel. Comparison of the present results with those of nickel on another support material is needed to help resolve this issue. Only one other study combining TPD and electron microscopy of nickel model-supported particles has appeared in the literature. Doering *et al.* (*14*) have investigated the desorption behavior of CO from nickel crystallites of varying average size supported on mica (muscovite). For increasing particle size from 1.6 to 5.4 nm, the CO molecular desorption peak temperature increased by ca. 20 K. Peak shifts presently observed are markedly greater than those observed due to particle size changes of nickel on mica, suggesting that particle size dependencies on CO adsorption strength are of secondary importance.

Evidence for Raft Formation

The transmission electron micrographs obtained after hydrogen reduction suggest that many of the nickel crystallites are present as small, thin particles. On the basis of microscopy alone, however, no estimate can be made of particle thicknesses.

The CO TPD results provide indirect evidence that nickel particles on titania may adopt a flat morphology. For mica-supported Ni, molecular desorption was accompanied by decomposition of CO, with the dissociation probability being greater for smaller Ni crystallites (*14*). It should be noted that the presence of potassium, one of the constituents of mica, increases CO dissociation probability on nickel under UHV-TPD conditions (*23*). Since CO adsorbs molecularly on low-index single-crystal Ni (*24–29*), but dissociatively on stepped Ni surfaces (*26*), Doering *et al.* concluded that CO dissociated at Ni surface defect sites, i.e., edge and corner sites of the particles. The density of these sites increases with decreasing crystallite size, consistent with the observed trend for CO dissociation probability. Spherical crystallites with diameters ranging from 2 to 3 nm (the average size estimated using electron microscopy) contain a substantial fraction of edge and corner atoms (*30*). However, no measurable CO dissociation took place on Ni particles of this size when supported on titania. If the crystallites were relatively flat, they would behave like low-index crystal planes and adsorb CO primarily in molecular form. The presence of titania adspecies at the defect sites of the nickel particles might also be expected to decrease CO dissociation probability.

Simoens *et al.* (*2*) have provided further independent evidence using ferromagnetic resonance (FMR) that a significant fraction of nickel crystallites are present on titania as thin crystallites following low or moderate-temperature reduction. Loss of ferromagnetic intensity following reduction was consistent with the formation of thin, nonferromagnetic particles less than 3 layers thick. It is important to note, however, that while the small nickel particles investigated in this study (ca. 2.5 nm in size) adopted a raft-like morphology, larger nickel particles may not. This would explain why raft-like Ni particles are not always observed on titania (e.g. (*31*)).

Nature of Interfacial Sites

The absence of CO dissociation on these low-surface-area Ni/TiO_2 samples provides limited information on the nature of so-called interfacial sites in catalysts exhibiting strong metal–support interactions. Burch and Flambard (*6–8*) have attributed the higher methanation activities of Group VIII metals supported on titania to the creation of special interfacial sites that are highly active for CO bond breaking. In their model, CO adsorbs at a metal–support interfacial site, with the carbon end bonded to a metal atom and the oxygen end bonded at the anion vacancy associated with an adjacent Ti^{3+} cation. Presumably in this configuration the adsorbed CO would be more susceptible to dissociation than CO associated with metal sites only.

The absence of CO dissociation under the UHV conditions of the TPD experiments suggests that if interfacial sites are indeed important, then either (i) C and/or O are bonded so strongly to the surface that they cannot recombine and do not desorb during the TPD experiments, (ii) the activation energy for CO dissociation remains greater than that for CO desorption (for equal preexponential factors for the two processes), or (iii) the number of CO dissociation sites is too small to detect with UHV-TPD measurements. With regard to the last possibility, transient isotope exchange studies of CO hydrogenation over Ni and other Group VIII metals have shown that only a small fraction of surface sites participates in the reaction (*32–36*). Thus, while the present findings do not show evidence for the existence of special interfacial sites, they do not necessarily rule out the model of Burch and Flambard.

Diffusion and Transport Processes

Diffusion and transport processes that might be important in model titania-supported catalysts during thermal treatment include particle sintering, migration of suboxides of titania onto the metal particles,

and metal particle diffusion into the oxide support.

Based on the electron micrographs of the model-supported nickel samples, as well as the CO TPD as a function of reduction temperature, it appears that titania-supported nickel particles are relatively resistant to sintering. Two adsorption/desorption cycles (with a maximum temperature of 650 K) following nickel deposition attenuated the CO signal evolving from Ni sites by less than 20%. Extended reduction at 820 K gave nickel particles of 2.5 nm average size. In contrast, for nickel particles supported on mica, two flash desorption cycles increased 3-nm particles ca. 40% in average size, and decreased the CO desorption signal by 40% (*14*). Further thermal treatments continued to change particle morphologies and increase the Ni particle size. Indeed, titania has previously been reported to inhibit particle sintering relative to other support materials (1).

Indirect evidence about the presence of titania adspecies on the nickel surface as well as the surface concentration of these species can be obtained through comparison of the present results with those recently reported for CO and H_2 TPD from nickel surfaces containing varying amounts of titania (*18*).

The CO desorption trace from a saturation CO coverage on the titania surface containing 0.2-nm Ni (which had been previously reduced in hydrogen at 650 K for 120 s, and shown in Fig. 1) is very similar to the trace from a nickel surface containing ca. 0.7 monolayers of titania (*18*). This suggests that the Ni particles on the former sample contain a significant concentration of titania adspecies. Larger Ni crystallites (thicker original Ni overlayers) appear to have progressively lower concentrations of titania adspecies for equivalent treatment conditions. For example, the ratio of the CO and H saturation coverages and the CO sticking coefficient for a 10-nm Ni on titania sample reduced at 650–720 K suggest that nickel particles contain an average titania concentration of ca. 0.1–0.2 monolayers.

The decrease in the initial sticking coefficient of CO, S_0, and the increase in the CO : H ratio at saturation coverages on the 1-nm Ni/TiO_2 sample with increasing reduction temperature suggests that migration of titania moieties onto the surfaces of the nickel particles takes place. Previous results have shown decreases in S_0 and increases in the CO : H ratio when increasing concentrations of titania adspecies were deposited on a nickel foil (*18*). Bartholomew and co-workers (*36*) have observed a similar dependence in the ratio of CO and H_2 uptakes on high-surface-area titania-supported nickel catalysts for progressively higher reduction temperatures.

For reduction temperatures higher than or equal to 770 K, the CO adsorption capacity on Ni sites was reduced significantly. Electron micrographs of the Ni/TiO_2 samples following 820 K reduction did not show a large loss of nickel surface area. *Ex situ* XPS analysis of the sample used in the TPD studies indicated that very little nickel was present near the surface. This apparent discrepancy between the TPD/XPS and the TEM studies can be rationalized in terms of different reducibilities of the two different supports. For the electron microscopy samples, removal of oxygen from the titania lattice to the gas phase must occur for reduction of the support to take place. For the TPD samples, an additional mechanism for TiO_2 reduction exists, as discussed elsewhere (*12*). This mechanism involves Ti cation diffusion from the underlying metallic titanium backing. Under UHV-TPD conditions this latter mechanism predominates, leading to higher reduction rates than would be observed in the absence of the metallic Ti substrate.

For electron microscopy samples similar to those used presently, Simoens *et al.* (*2*) reported significant sintering of nickel and loss of nickel from the support surface following reduction at 973 K. This was accompanied by a partial reduction of the titania support. It appears that a similar phenomenon occurred for the TPD samples but at a lower temperature. Evidently, reduction of the support plays an important role in the

diffusional processes which are responsible for these morphological changes. Reduction of the support could facilitate mobility of TiO_x species onto the metal.

CONCLUSIONS

The use of model-supported catalysts studied under ultrahigh vacuum conditions using TPD combined with electron microscopy allowed the following conclusions to be reached: (a) an electronic interaction between thin, supported nickel particles and *underlying* reduced titania weakens CO chemisorption on nickel; (b) electron micrographs and the lack of dissociative CO adsorption on nickel suggest that the nickel crystallites adopt a flat morphology; (c) no evidence exists for the formation of interfacial sites active for CO dissociation under UHV-TPD conditions; and (d) a variety of diffusional processes may occur during thermal treatment of a titania-supported catalyst and can lead to different configurations of the nickel.

ACKNOWLEDGMENTS

The generous support of Eastman–Kodak through a fellowship for one of us (G.B.R.) is gratefully acknowledged. Funding from the National Science Foundation was also received and is appreciated. Finally, we wish to thank Terry Hayden for assistance in the electron microscopy studies.

REFERENCES

1. Baker, R. T. K., Prestridge, E. B., and Garten, R. L., *J. Catal.* **56,** 390 (1979).
2. Simoens, A. J., Baker, R. T. K., Dwyer, D. J., Lund, C. R. F., and Madon, R. J., *J. Catal.* **86,** 359 (1984).
3. Tauster, S. J., Fung, S. C., and Garten, R. L., *J. Amer. Chem. Soc.* **100,** 170 (1978).
4. Horsley, J. A., *J. Amer. Chem. Soc.* **101,** 2870 (1979).
5. Herrmann, J. M., *J. Catal.* **89,** 404 (1984).
6. Burch, R., and Flambard, A. R., *J. Catal.* **78,** 389 (1982).
7. Burch, R., and Flambard, A. R., *J. Catal.* **85,** 8 (1984).
8. Bracey, J. D., and Burch, R., *J. Catal.* **86,** 384 (1984).
9. Santos, J., Phillips, J., and Dumesic, J. A., *J. Catal.* **81,** 147 (1983).
10. Resasco, D. E., and Haller, G. L., *J. Catal.* **82,** 279 (1983).
11. Meriaudeau, P., Dutel, J. F., Dufaux, M., and Naccache, C., *Stud. Surf. Sci. Catal.* **11,** 95 (1982).
12. Raupp, G. B., and Dumesic, J. A., *J. Phys. Chem.*, in press.
13. Ladas, S., Poppa, H., and Boudart, M., *Surf. Sci.* **102,** 151 (1981).
14. Doering, D. L., Dickinson, J. T., and Poppa, H., *J. Catal.* **73,** 91 (1982).
15. Raupp, G. B., and Dumesic, J. A., *J. Phys. Chem.* **88,** 660 (1984).
16. Udovic, T. J., and Dumesic, J. A., *J. Catal.* **89,** 314 (1984).
17. Tatarchuk, B. J., and Dumesic, J. A., *J. Catal.* **70,** 308 (1981).
18. Raupp, G. B., and Dumesic, J. A., *J. Catal.*, in press.
19. Kao, C. C., Tsai, S. C., Bahl, M. K., Chung, Y.-W., and Lo, W. J., *Surf. Sci.* **95,** 1 (1980).
20. Chung, Y.-W., Xiong, G., and Kao, C. C., *J. Catal.* **85,** 237 (1984).
21. Jiang, X.-Z., Hayden, T. F., and Dumesic, J. A., *J. Catal.* **83,** 168 (1983).
22. Hicks, R. F., Yen, Z.-J., and Bell, A. T., *J. Catal.* **89,** 498 (1984).
23. Kiskinova, M. P., *Surf. Sci.* **111,** 584 (1981).
24. Benziger, J. B., and Madix, R. J., *Surf. Sci.* **79,** 394 (1979).
25. Falconer, J. L., and Madix, R. J., *Surf. Sci.* **48,** 393 (1975).
26. Erley, W., and Wagner, H., *Surf. Sci.* **74,** 333 (1978).
27. Koel, B. E., Peebles, D. E., and White, J. M., *Surf. Sci.* **125,** 709 (1983).
28. Johnson, S. W., and Madix, R. J., *Surf. Sci.* **66,** 189 (1977).
29. Helms, C. R., and Madix, R. J., *Surf. Sci.* **52,** 677 (1975).
30. van Hardeveld, R., and Hartog, F., "Advances in Catalysis," Vol. 22, p. 75. Academic Press, New York, 1972.
31. Jiang, X. Z., Stevenson, S. A., Dumesic, J. A., Kelly, T. F., and Casper, R. J., *J. Phys. Chem.* **88,** 6191 (1984).
32. Happel, J., Suzuki, I., Kokayeff, P., and Fthenakis, V., *J. Catal.* **65,** 59 (1980).
33. Happel, J., Cheh, H. Y., Otarod, M., Ozawa, S., Severdia, A. J., Yoshida, T., and Fthenakis, V., *J. Catal.* **75,** 314 (1982).
34. Biloen, P., Helle, J. N., van den Berg, F. G. A., and Sachtler, W. M. H., *J. Catal.* **81,** 450 (1983).
35. Otarod, M., Ozawa, S., Yin, F., Chew, M., Cheh, H. Y., and Happel, J., *J. Catal.* **75,** 314 (1982).
36. Bartholomew, C. H., Pannell, R. B., and Butler, J. L., *J. Catal.* **65,** 335 (1980).